Journal of Multidisciplinary Engineering Science Studies (JMESS)
ISSN: 2458-925X
Vol. 7 Issue 11, November - 2021

Study The Performance Of Finned Pile Groups In Sand Under Cyclic Load Using Finite Element Modelling

Maher T. EL-Nemr[1]
Prof. of Geotechnical Engineering, Civil Engineering Department,
Menoufia University, Egypt,
E-mail: yos_el_nemr@hotmail.com.

Waseim R. Azzam[2]
Prof. of Soil Mechanics and Foundation, Structural Engineering Department,
Tanta University, Egypt,
E-mail:azzam_waseim@yahoo.com,
wassim.rajab@f-eng.tanta.edu.eg.

Ehab K. Gaber[3]
Lecture in Civil Engineering Department,
Menoufia University, Egypt,
E-mail: ehabkhirt@gmail.com,
ihab.khairt@sh.eng.menofia.edu.eg.

Omar Ashour[4]
Teaching assistant at Delta Higher Institute for Engineering and Technology, Civil Engineering Department,
Mansoura, Egypt,
E-mail: omarashour260@gmail.com,
omar.ashour@sh-eng.menofia.edu.eg.

***Abstract*—The driven finned pile is currently used as foundation type for high rise building, towers and offshore structures which constitute uplift loads. Finned pile was made by adding 4 welded plates around the end of the pile and this strategy was found to increase the uplift capacity of the pile. While the static capacity of the group finned piles is important, a secure design must also address issues of cyclic loading. Axial cyclic tension and compression load were implemented numerically for different spacing and different pile groups.**

This article presents a three-dimensional numerical model developed with the commercial finite element package, PLAXIS3D to analyze the impact of the cyclic loading on the finned pile group. All models were performed with constant number of fins, fin length, fin width, angle of fin with pile and the pile diameter to investigate the effect of cyclic load on finned pile groups. The effect of (D_r) (sand relative density) of 30, 50 and 80%, fin geometry and pile depth were investigated. As a result, Increasing the piles number affected on resistance under both tension and compression cyclic load significantly.

Keywords—Cyclic load, Group finned piles; Steel piles; Sand.

1. *Introduction*

Superstructure loads are often transferred to the stiffer underlying stratum using pile foundations. They are, in other words, members that offer support and load transfer from structure to another. A pile is a specific sort of column that can carry axial, lateral, and flexural loads with a variety of boundary conditions in the field. [4].

The loads transferred to the pile (due to railway and road traffic, wind and other factors) vary and can be absorbed as cyclic loadings on the piles. The behavior of the soil pile system evolves during the axial cyclic load on piles. [2].

An instrumented pile and centrifuge tests were devised to study the behavior of a pile foundation subjected to cyclic axial loading by [2]. During installation, cyclic loads and monotonic, the pile was designed to be placed in flight by jacking and could offer the pile's tip resistance and skin friction. To verify the proposed experimental approach, monotonic compression and tension tests were performed. The global reaction of the pile under cyclic loads is typical. Furthermore, several important properties connected to the pile's local responses in terms of cumulative displacement and load distribution.

The X-section concrete pile, cast-in-place, is a revolutionary foundation reinforcements technology with an X-shaped cross-section was investigated by [7]. Due to its bigger cross-sectional perimeter, an X-section pile with same cross-sectional area has greater side resistance than a standard circular pile. The behaviour of statically loaded X-section piles has received a lot of study, while the dynamic properties of X section piles have gotten less attention. This research describes a large-scale model test in sand for a circular pile and X section pile with the same cross-sectional area. The results of the experiments showed that axial cyclic load caused shaft friction and pile head stiffness to degrade. Load frequency and amplitude were used to determine the dynamic responses of an X section pile. Furthermore, a comparison of the circular pile and the X section pile

demonstrated that the X section pile can reduce cumulative settling and enhance shaft friction under cyclic stress. Even before to the vibration testing, a static load test was performed to determine the ultimate bearing capacity of such test piles. This research was supposed to serve as a good starting point for future research on the dynamic responses of X section piles in geotechnical engineering.

To examine the impact of cyclic axial loads on the performance of piled foundations, centrifuge modelling of pile groups and single piles was carried out by [9]. The effect of technique was studied, and it was discovered that the cyclic response of a pile with a correctly simulated jacked installation is substantially stiffer than that of a bored pile. The stiffness of the pile head decreases with such an increasing number of cycles but at a slower rate during displacement controlled axial cyclic load; during force controlled axial cyclic load, a bored pile accumulates more permanent settlement than a jacked pile. Individual piles in such a pile group subjected to axial cyclic loads perform similarly to single piles, indicating that there is no apparent group effect. Finally, centrifuge testing results verified a numerical analysis of axial loaded piles. The cyclic stiffness of soil increases considerably at the base of pre-jacked piles, but it remains nearly constant at the base of jacked piles.

Three-dimensional numerical model developed by [11], with FLAC3D to investigate the effects of changing the horizontal load's direction during the cycles. A typical scenario is a 1.7 m diameter and 10 m long pile established in dense homogenous sand. Force managed cycles with a change in lateral load direction have been implemented using a specific approach. With similar average and cyclic forces, the obtained results are compared with mono-directional lateral cyclic loads. The parametric latest results show the impact of the cyclic loading's average value and amplitude on the development of pile head horizontal displacements over time. When a multidirectional cyclic loading is applied, the deviating horizontal displacements are cumulative, and the resulting cumulative horizontal displacements are higher than when a mono-directional cyclic loading of the same amplitude is applied.

The method of finned piles in groups for improving uplift capacity of pile foundations subjected to cyclic loads has not been studied in previous literature. As a consequence, the goal of this research is to learn more about the behaviour of finned pile groups in sand under various cyclic loads.

2. *Research objective*

Since there are different types of tension piles, the paper focused on only one of them which is the tube pile with finned installed at the bottom end of the pile. The assembly comprised four evenly spaced fins welded around the perimeter at the bottom of the pile.

Therefore, the purpose of this study was to investigate numerically the effect of using finned pile groups, which has improved the pile-tension efficiency by providing positive anchorage near the bottom tip of the pile group. Also, finned piles are piles which has a fin at a given/ studied zone along the pile depth in sandy soil under cyclic loads, tension and compression, imposed on the pile cap. The numerical analysis using finite element modeling (FEM) and PLAXIS 3D Foundation software was employed to understand the improvement response of the modified piles under various cyclic loads. In addition to identify the failure pattern of such technique.

3. *Numerical Modeling*

A FEM was established for the finned pile groups using sandy soil. Before adopting the model, a parametric study comprising a numerical verification of the model was tested and validated as comparing with the data results provided from experimental prototype laboratory pile test.

One of the most effective approximate solutions that could be applied to solve geotechnical problems is the FE method [13]. In this research, numerical simulations were conducted using 3D FE software. The element stiffness matrix was created using a three-point Gaussian integration rule for all of the FE calculations, which were based on six-node triangular elements. The soil's failure behavior was defined using shear stress parameters. The Mohr–Coulomb model comprised five main parameters and was employed to simulate the elasto-plasticity of the soil. Most geotechnical engineers are associated with the model, which may be used to conduct simple testing on the soil samples.

In this research, the finned pile groups were simulated using PLAXIS 3D Foundation. At the bottom, the displacements were intended to be zero in both the (x and y directions) and in the (x direction) on the sides. An interfacial element of the interaction between the soil and both the pile and finned sections was adopted for all the embedment pile depths.

A preliminary elasto-plastic model was utilized in describing the interfacial behavior before simulating the interaction between the soil and the structure. (Rinter) the interface strength of 0.65 was taken as actual interfacial strength between the steel piles and soil. Three pairs of nodes were connected to the soil interfacial elements. The Newton–Cotes integration points were used to produce a stiffness matrix for the interfacial elements. By correlating the strength of the soil to an acceptable value for the strength reduction factor at the interface, a model for evaluating the interaction between the contact surfaces, the interface friction angle and adhesion was developed. The Coulomb criteria was used to distinguish between elastic interface behavior, which can result in minor displacements, and plastic interface

behavior, also known as slip. There are three means to obtain modulus of soil:

laboratory triaxial tests (derived from a soil tangent modulus calculation)

Pile-Load test

Based on previous experience, empirical correlations are made.

In this research the elastic modulus of soil was chosen according to empirical correlations based on previous experience [14.15.16].

4. Material properties and modeling

The pile and material modes, soil specifications, (optional for the behavior of materials in PLAXIS program software), interfaces, and stiffness characteristics are presented in Table (1) for the verification model.

Table (1): Materials Specifications, considered in the FE models (PLAXIS 3D Foundation)

Specification		Pile	Loose sand	Medium sand	Dense sand
Material model		Linear elastic	Mohr Coulomb	Mohr Coulomb	Mohr Coulomb
Material properties	γ (kN/m3)	78	16	16.6	18.4
	γsat (kN/m3)	78	16	16.6	18.4
	Dr (%)	-	30	50	80
Stiffness	E (kN/m2)	2.8 E7	4.5E4	7.5E4	10E4
	ν (nu)	0.3	0.35	0.35	0.35
Strength	C (kN/m2)	-	1	1	1
	φ (Phi)	-	30	36	40
	$\psi=(\varphi-30^{o})$ (dilation angle)	-	0	6	10
Interface	Rigidity (R_{inter})	-	0.65	0.65	0.65

5. Parametric study

The parameters were changed to see how they affected the finned pile groups' uplift capacity. All the details of the numerical models are presented in Table (2).

6. Results of Numerical Analysis

6.1. Verification of the Finite Element Model

For confirmation validation was done on the model test results. Where, prior to adopting the test for the aforementioned parametric study, a verification test held by [16] were tested and validated in comparison with the data results provided from there experimental prototype finned single pile test.

Medium-sized sand was used as the soil of maximum dry unit weight of (17.65 kN/m3), minimum dry unit weight of (14.65 kN/m3), effective diameter of (0.19 mm), uniformity coefficient of (2.6), percentage of fins of (1.8%) and specific gravity of (2.56). The sand bed in the soil tank was developed in 100 mm thick layers after the piles were erected. To ensure sand formation uniformity, a predetermined weight of sand was compacted into a certain volume within the soil bin with an accuracy of (0.001 kN) to achieve the desired relative density. A straight steel plate was used to level the generated sand.

The sand was compacted with a (40.0 N) hammer with a (200mm) diameter. After the experiment, three aluminum boxes measuring (50*50*30 mm) were implanted in the sand to recheck the relative density. The shear parameters of the studied soils were evaluated using drained triaxial sand tests in dense, medium, and loose situations. Three distinct relative densities (50,65, and 85 percent), were investigated in this study, yielding corresponding angles of internal friction from triaxial of (30,36, and 400) respectively. The pile was positioned at a predetermined depth before the sand bed was prepared, and the sand was installed to cover the pile length as mentioned above. For pile installation, this method is known as the quasi-non-displacement technique as stated by [16. 17]. As presented at Fig. 1.

All test series were conducted with a constant pile diameter (D) of 20 mm and fin length (Lf) (Lf= 6D= 120 mm), although fin width (b), embedded length of pile L, and inclination angle (b) varied.

In this research, single finned pile chosen to validate the experimental model. Same parameters (same pile type, very close sand type, fin inclination angle (900), number of fins (4) and fin-width diameter Ratio (0.5)), as shown previous, was modelled to validate the results. The test results for the model were verified using the PLAXIS 3D Foundation as a numerical program.

The comparison results, in term of pile/settlement response between this model and [16] model showed good agreement. With considering the simple difference. Fig. 2 (a and b) shows the results of this model, Pile load versus settlement curves, comparing with [16] results.

Table 2: Studied series in numerical analysis under cyclic load

Series	Constant parameters	Variable parameters	Load
1	Dr = 30% Dp = 2.5 cm Wf = 0.5 Dp, Lf = 2Dp No. of piles = 4 Spacing = 4Dp	Length per diameter ratio (L/d) = 10, 20 and 26	Cyclic Tension
2	Dr = 30% (L/d = 10) for pile Wf = 0.5 Dp, Lf = 2Dp No. of piles = 4	Spacing = 3Dp, 4Dp and 5Dp	
3	Dr = 30% (L/d = 10) for pile Wf = 0.5 Dp, Lf = 2Dp Spacing = 4Dp	No. of piles = 4, 5 and 6 piles	
4	Dp = 2.5 cm (L/d = 10) for pile Wf = 0.5 Dp, Lf = 2Dp No. of piles = 4 Spacing = 4Dp	Relative Density (Dr) = 30%, 50% and 80%	
5	Dr = 30% Dp = 2.5 cm Wf = 0.5 Dp, Lf = 2Dp No. of piles = 4 Spacing = 4Dp	Length per diameter ratio (L/d) = 10, 20 and 26	Cyclic Compression
6	Dr = 30% (L/d = 10) for pile Wf = 0.5 Dp, Lf = 2Dp No. of piles = 4	Spacing = 3Dp, 4Dp and 5Dp	
7	Dr = 30% (L/d = 10) for pile Wf = 0.5 Dp, Lf = 2Dp Spacing = 4Dp	No. of piles = 4, 5 and 6 piles	
8	Dp = 2.5 cm (L/d = 10) for pile Wf = 0.5 Dp, Lf = 2Dp No. of piles = 4 Spacing = 4Dp	Relative Density (Dr) = 30%, 50% and 80%	

Where (Dr) relative density of sand, (Lp) length of the pile, (Dp) diameter of pile, (Wf) fin width, (Lf) length of the fin and (L/ d) length per diameter ratio

It is clear that the finite element results follow the trend of the experimental data, resulting in moral agreement. Therefore, in the view of the fact that the adopted Plaxis 3d version is reliable for predicting the behavior of finned group piles under tension loads. It was decided to adopt this package for the analyses proposed in this manuscript.

Fig. 1: Test Tank and Finned Pile. [16].

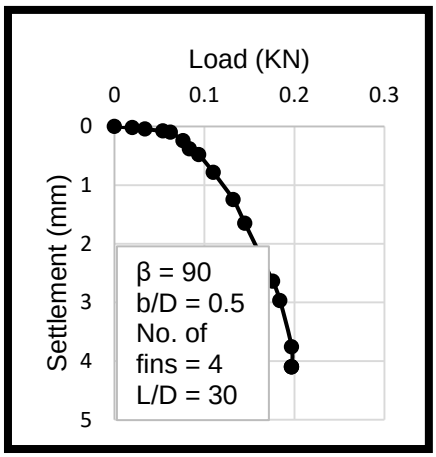

A: experimental model test results

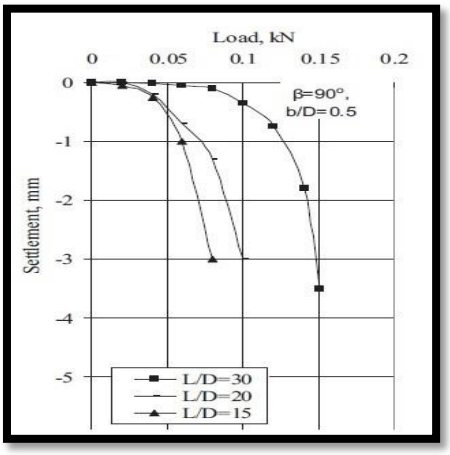

b: finite element analysis

Fig. 2: A comparison between load-settlement curves from experimental models after, [16] and Pile load versus settlement curve for single finned pile model in PLAXIS 3D.

6.2. Cyclic Tension Load

6.2.1. Effect of Spacing between Piles

To investigate the influence of different inter-pile spacing's on the finned pile groups under cyclic tension load, the time and acceleration are shown in Fig. 3. Also, the relation between Max. displacement and spacing between finned piles are shown in Fig. 4. In all the tests in this series, the relative density (Dr), pile length (Lp), diameter of the pile (Dp), width of the fin (Wf), length of the fin (Lf), length per diameter (L/d) ratio, and the number of piles were kept constant.

Also, it is evident that the displacement of the finned pile group decreases with an increase inter-pile spacing; the pullout capacity decreases from about 0.026 to 0.041 mm with increasing inter-pile spacing from 3 to 4 while it decreases from 0.041 to 0.065 mm when the spacing increases from 4 to 5.

From Figs. 3 and 4, the spacing between finned piles has a small effect under tension cyclic load.

6.2.2. Effect of Piles Number

To investigate the influence of piles number on the finned pile groups under cyclic tension load, the time and acceleration are shown in Fig. 5. Also, the relation between Max. displacement and spacing between finned piles are shown in Fig. 6. In all the tests in this series, the relative density (Dr), pile length (Lp), diameter of the pile (Dp), width of the fin (Wf), length of the fin (Lf), length per diameter (L/d) ratio, and the spacing between piles were kept constant.

Also, it is evident that the displacement of the finned pile group decreases with an increase piles number; the pullout capacity decreases from about 0.109 to 0.052 mm with increasing piles number from 4 to 5 while it decreases from 0.052to 0.042 mm when the number increases from 5 to 6.

From Figs. 5 and 6, increasing the piles number affected on resistance under tension cyclic load significantly.

6.2.3. Effect of Length per diameter ratio

To investigate the influence of length per diameter ratio on the finned pile groups under cyclic tension load, the time and acceleration are shown in Fig. 7. Also, the relation between Max. displacement and length per diameter ratio are shown in Fig. 8. In all the tests in this series, the relative density (Dr), pile length (Lp), diameter of the pile (Dp), width of the fin (Wf), length of the fin (Lf), piles number, and the spacing between piles were kept constant.

Also, it is evident that the displacement of the finned pile group decreases with an increase piles number; the pullout capacity decreases from about 0.109 to 0.01 mm with increasing piles number from 10 to 20 while it decreases from 0.01 to 0.008 mm when the number increases from 20 to 26.

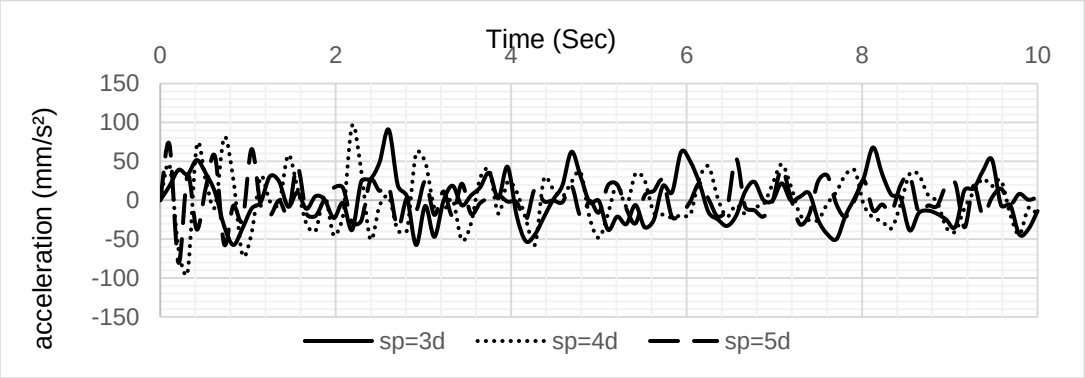

Fig. 3: Time – acceleration curve for different spacing between piles.

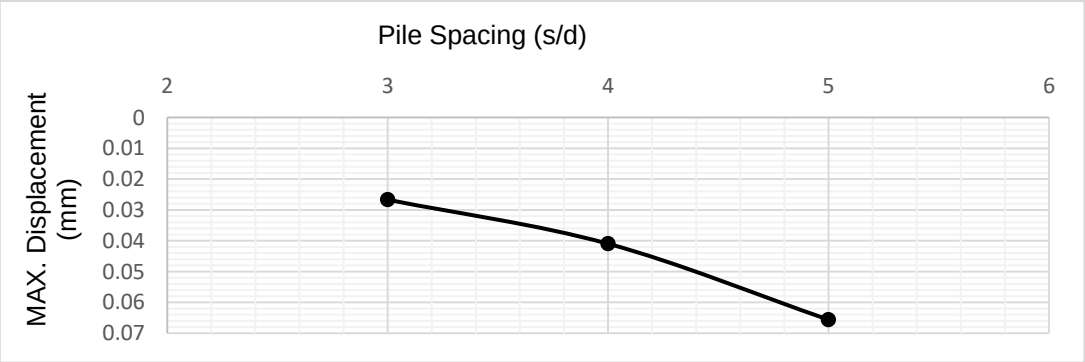

Fig. 4: Max. displacement curve for different spacing between piles.

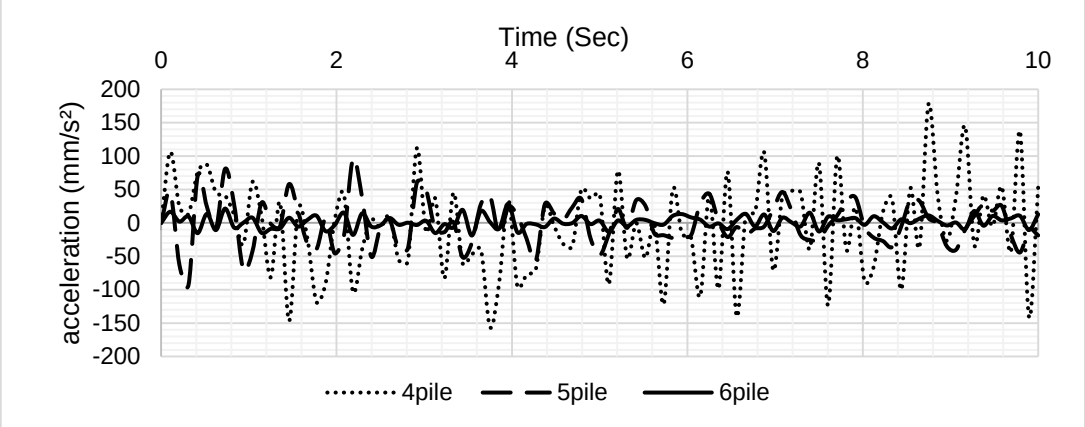

Fig. 5: Time – acceleration curve for different piles number.

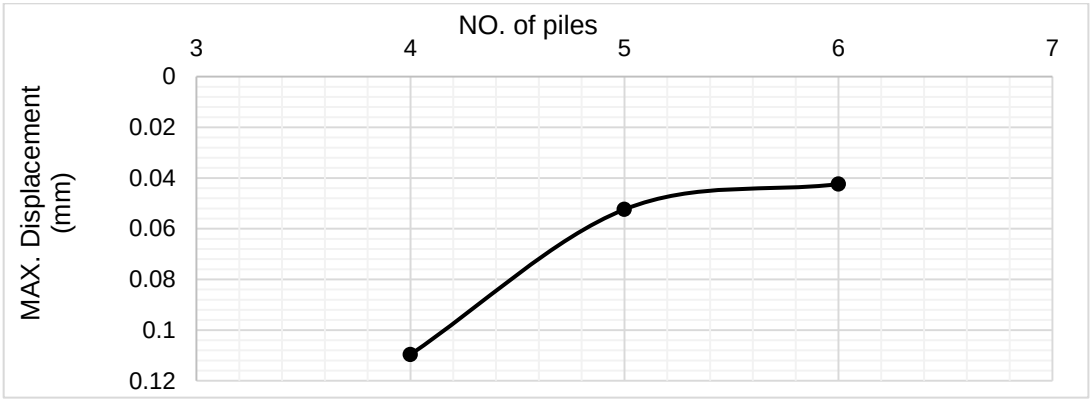

Fig. 6: Max. displacement curve for different piles number.

From Figs. 7 and 8, increasing the length per diameter ratio affected on resistance under tension cyclic load greatly from (L/d=10) to (L/d=20), but it has a little effect when it increases more than that value.

6.2.4. Effect of Relative Density

To investigate the influence of relative density on the finned pile groups under cyclic tension load, the time and acceleration are shown in Fig. 9. Also, the relation between Max. displacement and relative density are shown in Fig. 10. In all the tests in this series pile length (Lp), diameter of the pile (Dp), width of the fin (Wf), length of the fin (Lf), length per diameter ratio (L/d), piles number, and the spacing between piles were kept constant.

Also, it is evident that the displacement of the finned pile group decreases with an increase piles number; the pullout capacity decreases from about 0.109 to 0.065 mm with increasing piles number from 30 to 50 while it decreases from 0.065 to 0.04 mm when the number increases from 50 to 80.

From Figs. 9 and 10, increasing the relative density affected on resistance under tension cyclic load significantly.

6.3. Cyclic Compression Load

6.3.1. Effect of Spacing between Piles

To investigate the influence of different inter-pile spacing's on the finned pile groups under cyclic compression load, the time and acceleration are shown in Fig. 11. Also, the relation between Max. displacement and spacing between finned piles are shown in Fig. 12. In all the tests in this series, the relative density (Dr), pile length (Lp), diameter of the pile (Dp), width of the fin (Wf), length of the fin (Lf), length per diameter (L/d) ratio, and the number of piles were kept constant. increase inter-pile spacing; the pullout capacity decreases from about 0.027 to 0.043 mm with increasing inter-pile spacing from 3 to 4 while it decreases from 0.043 to 0.066 mm when the spacing increases from 4 to 5.

Also, it is evident that the displacement of the finned pile group decreases with an

From Figs. 11 and 12, the spacing between finned piles has a small effect under compression cyclic load.

6.3.2. Effect of Piles Number

To investigate the influence of piles number on the finned pile groups under cyclic compression load, the time and acceleration are shown in Fig. 13. Also, the relation between Max. displacement and spacing between finned piles are shown in Fig. 14. In all the tests in this series, the relative density (Dr), pile length (Lp), diameter of the pile (Dp), width of the fin (Wf), length of the fin (Lf), length per diameter (L/d) ratio, and the spacing between piles were kept constant.

Also, it is evident that the displacement of the finned pile group decreases with an increase piles number; the pullout capacity decreases from about 0.114 to 0.0534 mm with increasing piles number from 4 to 5 while it decreases from 0.0534 to 0.0435 mm when the number increases from 5 to 6.

From Figs. 13 and 14, increasing the piles number affected on resistance under compression cyclic load significantly.

6.3.3. Effect of Length per diameter ratio

To investigate the influence of length per diameter ratio on the finned pile groups under cyclic compression load, the time and acceleration are shown in Fig. 15. Also, the relation between Max. displacement and length per diameter ratio are shown in Fig. 16. In all the tests in this series, the relative density (Dr), pile length (Lp), diameter of the pile (Dp), width of the fin (Wf), length of the fin (Lf), piles number, and the spacing between piles were kept constant.

Also, it is evident that the displacement of the finned pile group decreases with an increase piles number; the pullout capacity decreases from about

0.115 to 0.0072 mm with increasing piles number from 10 to 20 while it decreases from 0.0072 to 0.0041 mm when the number increases from 20 to 26.

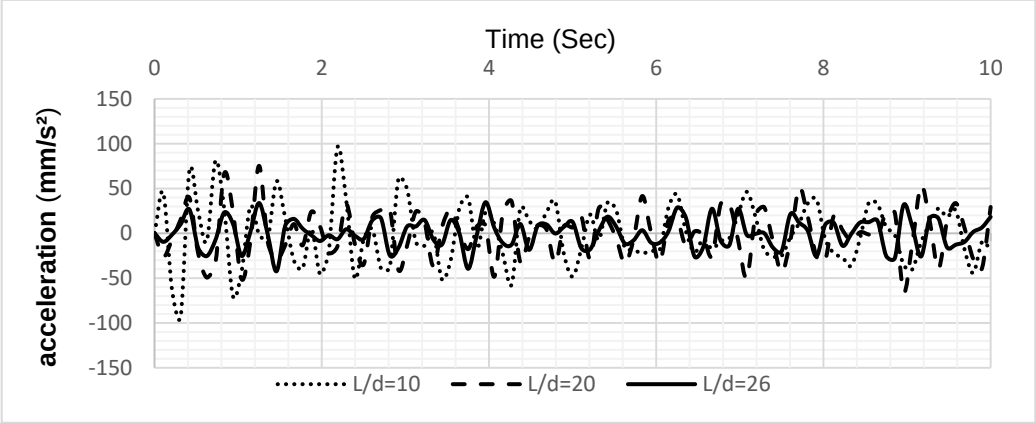

Fig. 7: Time – acceleration curve for different length per diameter ratio.

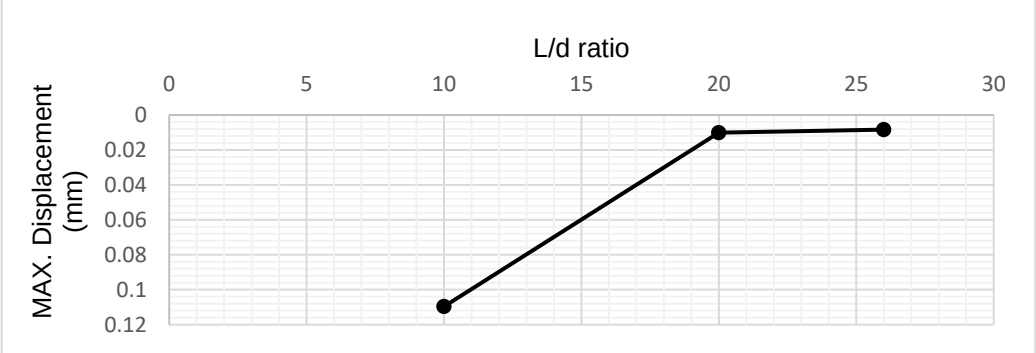

Fig. 8: Max. displacement curve for different length per diameter ratio.

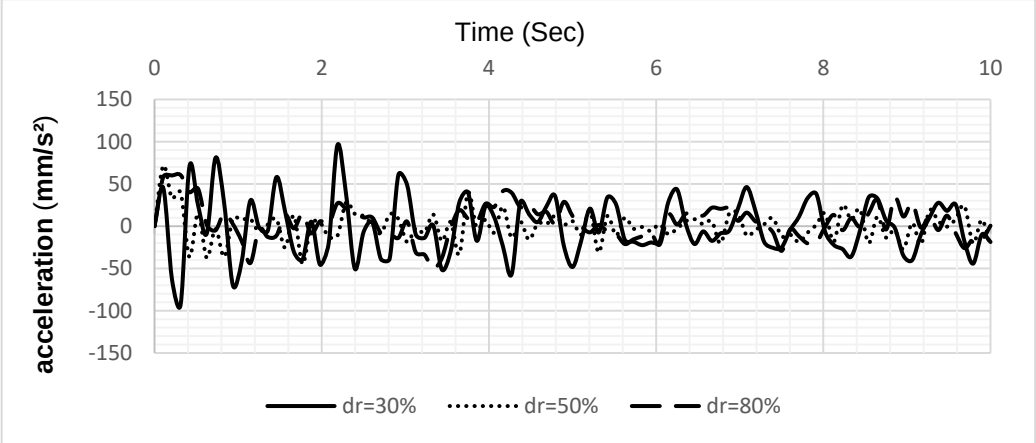

Fig. 9: Time – acceleration curve for different relative densities.

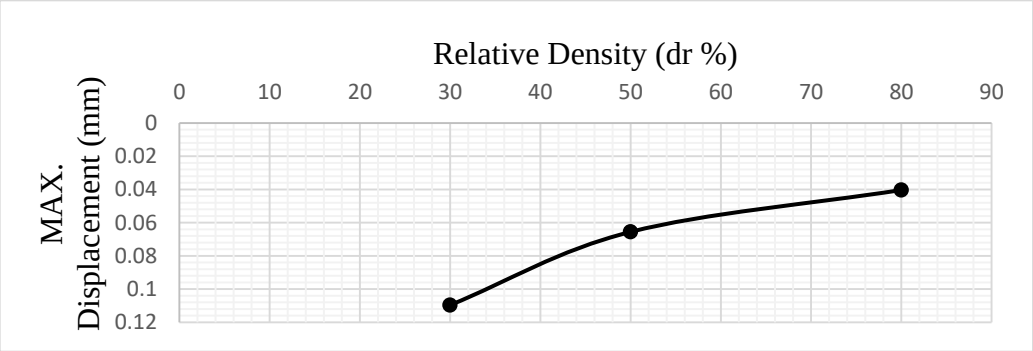

Fig. 10: Max. displacement curve for different relative densities.

From Figs. 15 and 16, increasing the length per diameter ratio affected on resistance under compression cyclic load greatly from (L/d=10) to (L/d=20), but it has a little effect when it increases more than that value.

6.3.4. Effect of Relative Density

To investigate the influence of relative density on the finned pile groups under cyclic compression load, the time and acceleration are shown in Fig. 17. Also, the relation between Max. displacement and relative density are shown in Fig. 18. In all the tests in this series pile length (Lp), diameter of the pile (Dp), width of the fin (Wf), length of the fin (Lf), length per diameter ratio (L/d), piles number, and the spacing between piles were kept constant.

Also, it is evident that the displacement of the finned pile group decreases with an increase piles number; the pullout capacity decreases from about 0.114 to 0.059 mm with increasing piles number from 30 to 50 while it decreases from 0.059 to 0.045 mm when the number increases from 50 to 80.

From Figs. 17 and 18, increasing the relative density affected on resistance under compression cyclic load significantly.

7. Conclusion

This research focused on determining the effect of finned pile groups under cyclic load. Both axial cyclic tension and compression load were implemented numerically with the commercial finite element package, PLAXIS3D to analyze the impact of the cyclic loading on the finned pile group. All models were performed under cyclic load with different parameters.

Based on both analyses in investigating the pile's group behaviors, the following conclusions were made:

- The spacing between finned piles has a small effect under tension cyclic load.
- Increasing the piles number affected on resistance under tension cyclic load significantly.
- Increasing the length per diameter ratio has a significant effect on resistance under tension cyclic load incredibly from (L/d=10) to (L/d=20), but it has a little effect when it increases more than that value.
- Increasing the relative density affected on resistance under tension cyclic load significantly.
- The spacing between finned piles has a small effect under compression cyclic load.
- Increasing the piles number affected on resistance under compression cyclic load significantly.
- Increasing the length per diameter ratio affected on resistance under compression cyclic load greatly from (L/d=10) to (L/d=20), but it has a little effect when it increases more than that value.
- increasing the relative density affected on resistance under compression cyclic load incredibly.

Acknowledgment

This study is based on a Ph.D. thesis being prepared by a fourth author, under the supervision of the authors.

References

1 Hededal, O., & Klinkvort, R. T. A New Elasto-Plastic Spring Element for Cyclic Loading of Piles Using the P-Y Curve Concept. In Numerical Methods in Geotechnical Engineering: NUMGE 2010 (1 ed., Vol. 1, pp. 883-888). Trondheim: Taylor and Francis Group. (2010).

2 Alain Le Kouby, Julio Rakotonindriana, Luc Thorel. Load Distribution Along a Pile - Case of Cyclic Axial Loading. EUROFUGE 2016, 3rd European conference on Physical Modelling in Geotechnics, Jun, NANTES, France. pp.257-

262. hal-01358234. (2016).

3 LeBlanc, C., Houlsby, G. T., & Byrne, B. W. Response of Stiff Piles in Sand to Long-term Cyclic Lateral Loading. Géotechnique, 60(2), 79-90. (2010).

4 El-Nemr, A. M., Ashour, O., & Hekal, G. M. Dynamic Response of Confined Concrete Piles with FRP Tubes in Sandy Soil Using Finite Element Modeling. Insights and Innovations in Structural Engineering, Mechanics and Computation – Zingoni (Ed.) © 2016 Taylor & Francis Group, London, ISBN 978-1-138-02927-9. (2016).

5 Zhou, W., Wang, L., Guo, Z., Liu, J., & Rui, S. A Novel tz Model to Predict the Pile Responses Under Axial Cyclic Loadings. Computers and Geotechnics, 112, 120-134. (2019).

6 Costa D'Aguiar, S., Modaressi, A., Alberto dos Santos, J., & Lopez-Caballero, F. Piles Under Cyclic Axial Loading: Study of The Friction Fatigue and Its Importance in Pile Behavior. Canadian geotechnical journal, 48(10), 1537-1550. (2011).

7 Lu, Y., Liu, H., Zheng, C., & Ding, X. Experimental Study on the Behavior of X-Section Pile Subjected to Cyclic Axial Load in Sand. Shock and Vibration, (2017).

8 Zhang, B. J., Huang, B., Mei, C., Fu, X. D., Luo, G., & Yang, Z. J. Dynamic Behaviors of a Single Soft Rock-Socketed Shaft Subjected to Axial Cyclic Loading. Advances in Materials Science and Engineering, (2016).

9 Li Zheming, Bolton Malcolm D., and Haigh Stuart K. Cyclic Axial Behavior of Piles and Pile Groups in Sand. Canadian Geotechnical Journal. 49(9): 1074-1087. https://doi.org/10.1139/t2012-070. (2012).

10 Muhammed, R. D., Canou, J., Dupla, J. C., & Tabbagh, A. Evaluation of Local Soil-Pile Friction in Saturated Clays Under Cyclic Loading. *Soils and Foundations*, *58*(6), 1299-1312. (2018).

11 Jenck, O.; Obaei, A.; Emeriault, F.; Dano, C. Effect of Horizontal Multidirectional Cyclic Loading on Piles in Sand: A Numerical Analysis. J. Mar. Sci. Eng. 2021, 9, 235. https://doi.org/10.3390/jmse9020235, (2021).

12 Page, A. M., Klinkvort, R. T., Bayton, S., Zhang, Y., & Jostad, H. P. A Procedure for Predicting the Permanent Rotation of Monopiles in Sand Supporting Offshore Wind Turbines. Marine Structures, 75, 102813, (2021).

13 Han et al. J. Geomech., Modeling behavior of friction pile in compacted glacial till Int. 10.1061/(ASCE)GM .1943-5622.0000659, D4016009, (2016).

14 A. Sallam, Behavior of Grouted Screw Piles Under Inclined Loads in Sand, A THESIS Submitted for the Degree of Master of Philosophy in Civil Engineering (Structural Engineering), Faculty of Engineering - Tanta University, (2016),

15 Ghaly A. et al, Model Investigation of the Performance of Single Anchors and Groups of Anchors, Canadian Geotechnical Journal, Vol. 31, No. 2, pp. 273-284, (1994).

16 W. Azzam and A. Elwakil, Model Study on the Performance of Single-Finned Pile in Sand under Tension Loads, paper is part of the International Journal of Geomechanics, ©ASCE, ISSN 1532-3641, (2016).

17 Fioravante, et al., On the effects of Residual Tangent Stresses in Centrifuge Pile Tests, Proc.,6thInt. Conf. on Physical Modelling in Geotechnics, Taylor & Francis, Leiden, the Netherlands, 827–833, (2006).

18 K. Gaaver, Alexandria Engineering Journal, Uplift Capacity of Single Piles and Pile Groups Embedded in Cohesionless soil, Volume 52, Issue 3, Pages 365-372, (2013).

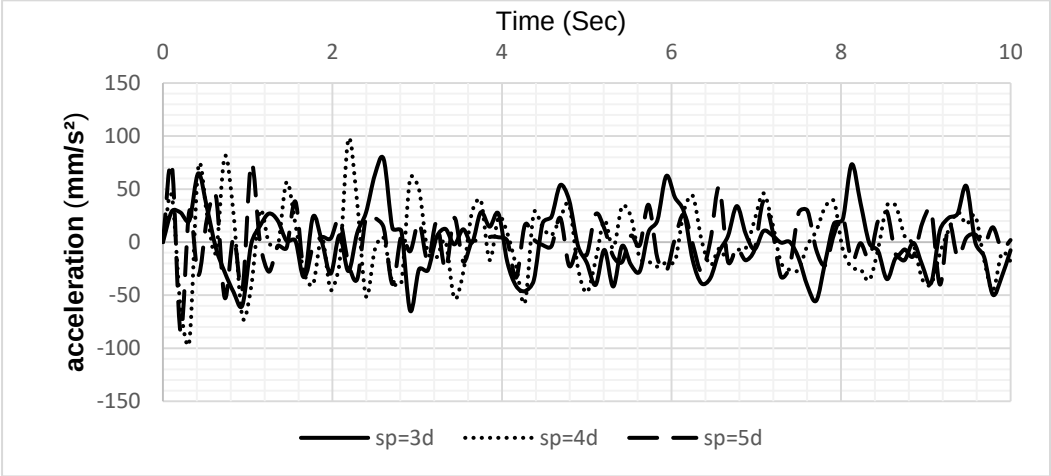

Fig. 11: Time – acceleration curve for different spacing between piles.

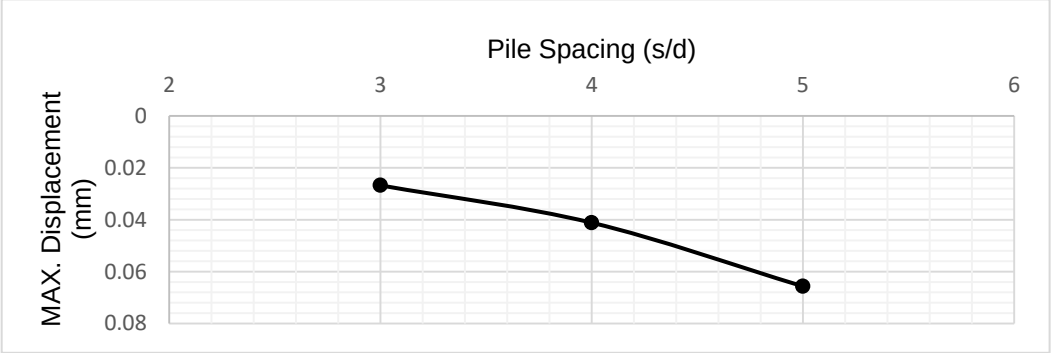

Fig. 12: Max. displacement curve for different spacing between piles.

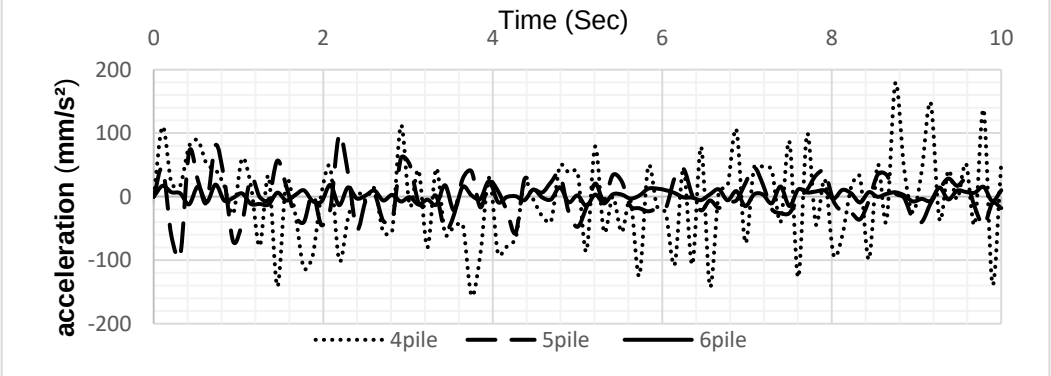

Fig. 13: Time – acceleration curve for different piles number.

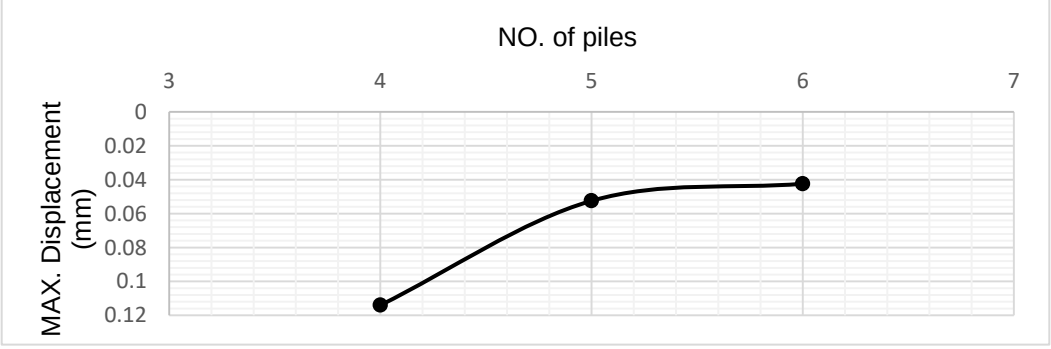

Fig. 14: Max. displacement curve for different piles number.

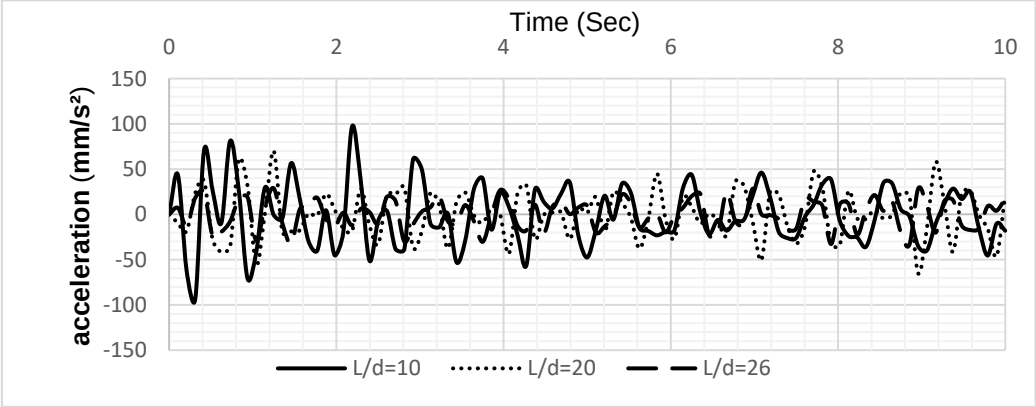

Fig. 15: Time – acceleration curve for different length per diameter ratio.

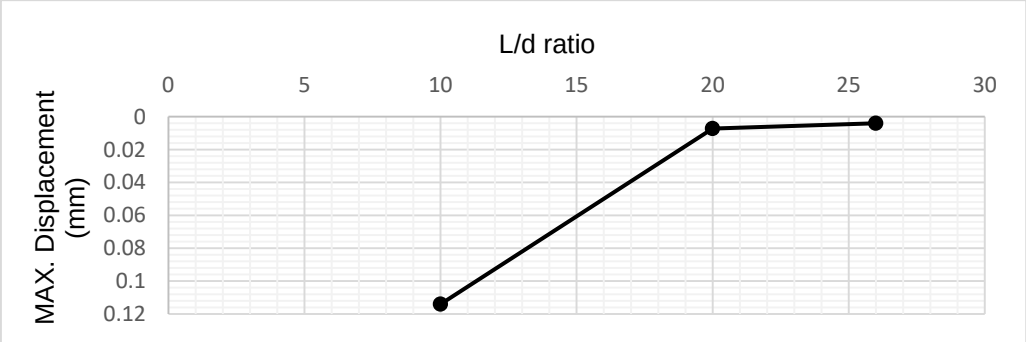

Fig. 16: Max. displacement curve for different length per diameter ratio.

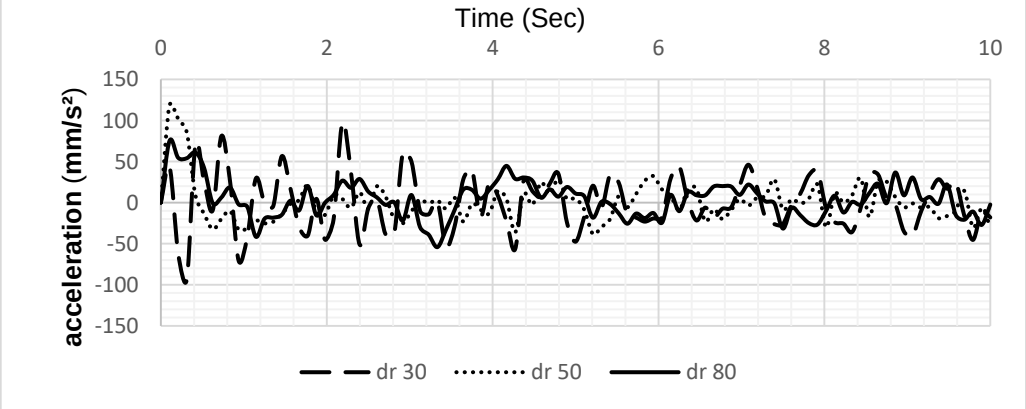

Fig. 17: Time – acceleration curve for different relative densities.

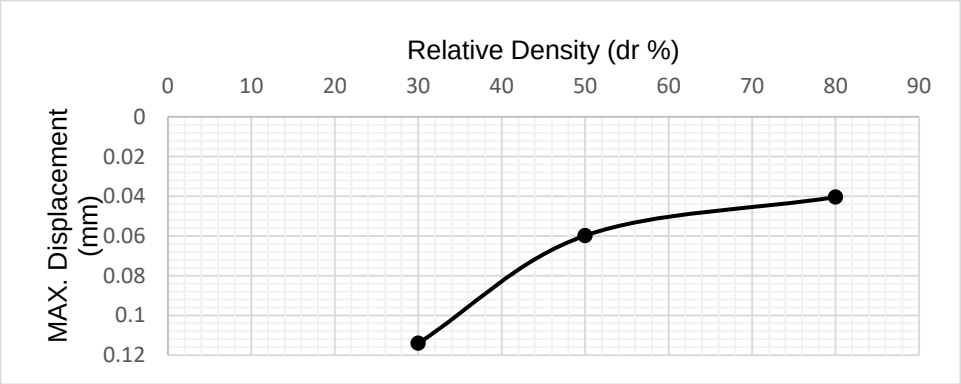

Fig. 18: Max. displacement curve for different relative densities.

Symbols:

Dp	Diameter of the pile;	Lp	Length of the pile;
D_r	Relative density of soil;	E_b	Modulus of Elasticity of material
G	Specific gravity for the soil;	C	Cohesion of soil;
L/d	Length/diameter ratio;	D_{10}	Particle size at 10% finer.;
Lf	Fin length;	D_{30}	Particle size at 30% finer.;
SW	well-graded sand	D_{60}	Particle size at 60% finer.;
Cu	Uniformity Coefficient;	Cc	Coefficient of curvature;
K_{ST}	relative stiffness of the soil-foundation system	E_s	Modulus of Elasticity of soil
R^2	Coefficient of determination;	***Greek letter***	
R_{inter}	Rigidity;	γ	Unit weight of soil;
S/D	Spacing/Diameter ratio;	φ°	Angle of internal friction;
Wf	Fin widths;	ψ	Dilation angle;
Abbreviations			
FEM	Finite element modeling;	USCS	Unified Soil Classification System.